Stability of Self-Focused Filaments in Laser-Produced Plasmas

The filamentation instability causes local intensity maxima in a laser beam propagating through a plasma to self-focus to high intensities. This process can affect many aspects of the beam propagation and absorption, so it has long been a subject of interest in laser–plasma interaction research. The theoretical thresholds and growth rates for the linear phase of the filamentation instability are readily determined analytically.[1] As the instability develops beyond the linear phase and the filament becomes smaller and more intense, the self-focusing effect is counterbalanced by diffraction. This leads to the possibility of a nonlinear inhomogeneous equilibrium—a steady-state, high-intensity, low-density filament in which the plasma pressure outside is balanced by the ponderomotive force of the light inside. This nonlinear phase of the instability, which produces the highest intensities and is therefore of the greatest practical interest, is difficult to treat analytically because of the strong density and intensity inhomogeneities associated with such a filament. The nonlinear stage of filamentation is usually studied using simulation codes that directly integrate the equations of motion for the fields and particles or fluids.[2] One important problem that is difficult to study in this way, however, concerns the long-term stability of the nonlinearly saturated filament, once formed. A stable filament would have a greater influence on absorption nonuniformity and on beam bending[3]—important considerations for direct- and indirect-drive laser-fusion schemes, respectively. It would also be expected to make a greater contribution to parametric instabilities.[4–6] An investigation of the stability of a filament through simulation would require the simulation to cover a large spatial extent of plasma over a long period of time. At present, due to computational limitations,[7] such extensive simulations necessitate some approximations in the equations used to describe the filament, in particular the paraxial approximation to the wave equation for the light propagation. This approximation requires that the propagating light not develop wave-vector components that deviate far from the initial direction of the beam. Recent studies[8] indicate, however, that the filaments most likely to be stable are very intense and have very small radii, of the order of the light wavelength, so that the paraxial approximation is questionable. Moreover, a simulation can treat only one specific set of irradiation and plasma parameters at a time, and extrapolating from simulations based on a limited sampling of parameter space to general results on stability is problematic.

A purely analytic approach to filament stability requires many approximations and idealizations to render the problem at all tractable; for this reason applying the few results that have been obtained analytically to realistic filaments is difficult. These results do suggest, however, that filaments may be unstable to kinking or bending perturbations[9] and to necking or "sausage" perturbations,[10] with the latter having a faster growth rate.

In this article the stability problem of a realistic filament will be addressed for the first time using a semi-analytic approach. A dispersion relation is obtained that describes the linear growth of a sausage-type perturbation of a self-consistent, self-focused cylindrical filament in equilibrium. This dispersion relation is analogous to the simple polynomial dispersion relations obtained for the instabilities of a plane electromagnetic wave in a homogeneous plasma.[11] Rather than being a polynomial in the perturbation wave number and frequency as in the homogeneous case, however, the filament dispersion relation depends on these quantities through ordinary differential equations that must be solved numerically for each value of the frequency and wave number. This is still much easier than the simultaneous solution of several coupled partial differential equations as required by a simulation, yet it allows the consideration of a physically realistic filament equilibrium, arbitrarily long space and time intervals, and the use of the full wave equation to describe the light propagation.

We will show that filament stability depends crucially on filament size. First, consider the case where the filament is small enough that only one waveguide mode will propagate. The pump (laser) light propagates through the filament in this fundamental mode at frequency ω_0 and axial wave number k_0. Amplitude modulation (sausaging) results from adding a perturbing light wave in the same mode at a differing frequency

$\omega_0 + \Delta\omega$ and wave number $k_0 + \Delta k$, $\Delta\omega$ and Δk being related by the dispersion relation for the waveguide mode. This intensity modulation itself has frequency $\Delta\omega$ and wave number Δk and tends to move along the filament at the waveguide group velocity $\Delta\omega/\Delta k$, which in general is comparable to the speed of light. Because the speed of the perturbation greatly exceeds the ion-sound speed, the perturbation interacts weakly with the surrounding plasma, limiting potential growth rates. A much stronger interaction can be expected if the filament is large enough to allow two or more waveguide modes to propagate. In this case the perturbing light can be in a second mode with a different dispersion relation. Thus, it can have a frequency $\omega_1 \cong \omega_0$ but a significantly smaller axial wave number $k_1 < k_0$, so that $\Delta\omega/\Delta k = (\omega_0 - \omega_1)/(k_0 - k_1)$ is much smaller than the speed of light and can be comparable to the ion-sound speed, leading to an enhanced interaction.

To explore these ideas quantitatively, we consider an equilibrium filament consisting of a low-density cylindrical channel in a higher-density homogeneous background plasma. The channel is formed by the ponderomotive pressure of light propagating within the channel in the fundamental waveguide mode. Assume that in equilibrium the axis of the filament lies in the z direction and the filament intensity and density vary only as a function of r. Write the electric field E_0 of the pump wave as

$$\frac{e}{v_T m\omega_0} E_0(r,z,t) = \psi_0(r) e^{i(k_0 z - \omega_0 t)} + \text{c.c.}, \qquad (1)$$

so that ψ_0 represents the oscillatory velocity $v_0 = eE_{\max}/m\omega_0$ normalized to v_T, the electron thermal velocity. The pump satisfies the wave equation in cylindrical geometry

$$\left[c^2\left(\frac{d^2}{dr^2} + \frac{1}{r}\frac{d}{dr}\right) + \omega_0^2 - \omega_{p0}^2(r) - c^2 k_0^2\right]\psi_0(r) = 0, \qquad (2)$$

with boundary conditions $\psi_0(r) \to 0$ as $r \to \infty$, $(d\psi_0/dr)_{r=0} = 0$ for a bound-state waveguide mode propagating in a cylindrical filament. The square of the plasma frequency $\omega_{p0}^2(r)$ is proportional to the density, which is determined by pressure balance with the ponderomotive force of the pump:

$$\frac{\omega_{p0}^2(r)}{\omega_0^2} = \frac{n_0(r)}{n_c} = \frac{N_0}{n_c} e^{-\frac{1}{4}\psi_0^2(r)}, \qquad (3)$$

where N_0 is the background density outside the filament and n_c is the critical density. Equations (2) and (3) give a nonlinear differential equation for ψ_0, which together with the boundary conditions results in an eigenvalue problem determining k_0, ψ_0, and the filament density profile $n_0(r)$. The pump propagates in the fundamental mode; however, if the filament is deep and wide enough, higher-order waveguide modes will also propagate in it. These eigenmodes satisfy the equation

$$\left[\frac{d^2}{ds^2} + \frac{1}{s}\frac{d}{ds} - \frac{n_0(s)}{n_c}\right]\phi_j(s) = \Gamma_j \phi_j(s), \qquad (4)$$

where $j = 0$ represents the fundamental mode, $s \equiv \omega_0 r/c$, and the eigenvalue Γ_j determines the relation between the axial wave number k_j of the eigenmode and its frequency $\omega_j : c^2 k_j^2/\omega_0^2 - \omega_j^2/\omega_0^2 = \Gamma_j$. In general, the spectrum of eigenvalues Γ_j will contain discrete values for bound modes with $\Gamma_j - N_0/n_c$ and a continuum of unbound modes with $\Gamma_j - N_0/n_c$. Since we are interested in instability, we will be primarily concerned with the bound modes; the unbound modes propagate away from the filament before they have an opportunity to grow significantly. The eigenfunctions are orthogonal and assumed normalized to unity. The pump is assumed proportional to the fundamental eigenmode: $\psi_0(s) = \alpha_0\phi_0(s)$, where α_0 may be taken real and represents the pump amplitude.

We employ fluid equations for the plasma density; linearizing n around the equilibrium density profile $n_0(r)$ results in an inhomogeneous driven wave equation for the density perturbation $n_1(r,z,t)$:

$$\frac{\partial^2 n_1}{\partial t^2} - c_s^2\left\{\nabla^2 n_1 - \frac{\nabla n_0}{n_0}\cdot\nabla n_1 + \left[\frac{(\nabla n_0)^2}{n_0^2} - \frac{\nabla^2 n_0}{n_0}\right]n_1\right\}$$

$$= -\frac{Z}{M}\left[n_0\nabla\cdot\mathbf{F}_p + (\nabla n_0)\cdot\mathbf{F}_p\right], \qquad (5)$$

where c_s is the ion acoustic speed, Z and M are the ion charge and mass, respectively, and $\mathbf{F}_p$ is the ponderomotive force resulting from the electromagnetic waves.

The density perturbation n_1 is assumed to have real wave number k in the z direction (along the filament) and frequency ω, which may be complex: $n_1(r,z,t) = n(r)e^{i(kz-\omega t)} + \text{c.c.}$ The interaction of the density perturbation with the pump generates a perturbed electromagnetic wave:

$$\psi_1(r,z,t) = \left\{\psi_+(r)e^{i\left[(k+k_0)z-(\omega+\omega_0)t\right]} + \psi_-(r)e^{i\left[(k-k_0)z-(\omega-\omega_0)t\right]}\right\} + \text{c.c.},$$

where, since the frequency ω may be much smaller than ω_0, both upshifted and downshifted terms are kept. The linearized wave equation then becomes

$$\left[\frac{d^2}{ds^2} + \frac{1}{s}\frac{d}{ds} + \left(1 \pm \frac{c_s}{c}\Omega\right)^2 - \left(\kappa_0 \pm \kappa\right)^2 - \frac{n_0(s)}{n_c}\right]\psi_\pm(s) = \frac{n(s)}{n_c}\psi_0(s). \tag{6}$$

The first-order ponderomotive force resulting from the beating of the pump and perturbed electromagnetic waves is

$$\begin{aligned}\mathbf{F}_p &= -mv_T^2\nabla\left(\psi^2\right)_1 \\ &= -mv_T^2\,\nabla\left\{\left[\psi_0^*(s)\psi_+(s)+\psi_0(s)\psi_-(s)\right] \times e^{i(\kappa\zeta-\Omega\tau)} + \text{c.c.}\right\}.\end{aligned} \tag{7}$$

In Eqs. (6) and (7) we have introduced the dimensionless quantities $\Omega = \omega c/\omega_0 c_s$, $\kappa = \omega_0 k/c$, $\varsigma = \omega_0 z/c$, and $\tau = c_s\omega_0 t/c$. Substituting Eq. (7) into Eq. (5), we obtain an equation for the perturbed density in terms of the perturbed electromagnetic fields:

$$\begin{aligned}&\left[\frac{d^2}{ds^2} + \left(\frac{1}{s} - \frac{1}{n_0}\frac{dn_0}{ds}\right) + \Omega^2 - \kappa^2 + \frac{1}{n_0^2}\left(\frac{dn_0}{ds}\right)^2 - \frac{1}{n_0}\frac{d^2n_0}{ds^2} - \frac{1}{n_0}\frac{1}{s}\frac{dn_0}{ds}\right]\frac{n(s)}{n_c} \\ &= -\frac{n_0(s)}{n_c}\left[\frac{d^2}{ds^2} + \left(\frac{1}{s} + \frac{1}{n_0}\frac{dn_0}{ds}\frac{d}{ds}\right) - \kappa^2\right] \times \left(\psi_0\psi_+ + \psi_0\psi_-\right).\end{aligned} \tag{8}$$

It is useful to expand the electromagnetic fields in terms of the orthonormal eigenfunctions $\phi_j(s)$ of Eq. (4):

$$\psi_\pm(s) = \sum_{j=1}^{\infty}\beta_j^\pm\phi_j(s).$$

Defining $\eta_j(s)$ as the solution of

$$\begin{aligned}&\left[\frac{d^2}{ds^2} + \left(\frac{1}{s} - \frac{1}{n_0}\frac{dn_0}{ds}\right)\frac{d}{ds} + \Omega^2 - \kappa^2 + \frac{1}{n_0^2}\left(\frac{dn_0}{ds}\right)^2 - \frac{1}{n_0}\frac{d^2n_0}{ds^2} - \frac{1}{n_0}\frac{1}{s}\frac{dn_0}{ds}\right]\eta_j(s) \\ &= -\frac{n_0(s)}{n_c}\left[\frac{d^2}{ds^2} + \left(\frac{1}{s} + \frac{1}{n_0}\frac{dn_0}{ds}\right)\frac{d}{ds} - \kappa^2\right]\phi_0(s)\phi_j(s),\end{aligned} \tag{9}$$

satisfying the boundary conditions $\eta_j'(0) = 0$ and outgoing waves as $s \to \infty$, we see from Eq. (8) that the density perturbation can be written as

$$\frac{n(s)}{n_c} = \alpha_0\sum_j\left(\beta_j^+ + \beta_j^-\right)\eta_j(s). \tag{10}$$

Combining Eqs. (6) and (10) then gives a linear relation among the coefficients $\beta_j^\pm$:

$$\left[\left(1 \pm \frac{c_s}{c}\Omega\right)^2 - 1 - \left(\kappa_0 \pm \kappa\right)^2 + \Gamma_j\right]\beta_j^\pm = \alpha_0^2\sum_{j'}\left(\beta_{j'}^\pm + \beta_{j'}^\mp\right)L_{jj'}, \tag{11}$$

where the $L_{jj'}$ denote the integrals over the wave functions: $L_{jj'} = \int_0^\infty \phi_j(s)\eta_{j'}(s)\phi_0(s)s\,ds$.

While the sums in Eq. (11) extend over an infinite range of j, only the finite number of discrete bound states are of interest in studying instabilities, and in small filaments only a few of these may exist. Truncating the sums in Eq. (11) to the bound states leads to a finite set of linear homogeneous equations in the $\beta_j^\pm$, and setting the determinant of the coefficients to zero gives a dispersion relation relating Ω and κ. Unlike the homogeneous case, however, this dispersion relation is not a polynomial but a more complicated function of Ω and κ, since the coefficients $L_{jj'}$ depend on Ω and κ through the solutions of the differential equation (9). These solutions are readily obtained numerically, however, allowing the evaluation of the dispersion relation and the determination of the unstable modes of the filament and their growth rates.

As an example, consider a background plasma with a uniform density of half-critical, $N_0/n_c = 0.5$, and an ion sound speed of $c_s = 10^{-3}\,c$, corresponding to an electron temperature of approximately 1 keV. For a given central field amplitude $\psi_0(0)$, the filament density and intensity profiles are found by integrating Eqs. (2) and (3), adjusting the axial wave number k_0 so that the boundary conditions are satisfied. The waveguide modes are then found from Eq. (4). At this density and temperature a central intensity of $\psi_0(0) \equiv v_0/v_T = 7$ is found to be sufficient to produce a filament wide enough to allow two electromagnetic modes to propagate. The resulting pump field amplitude and filament density profile are shown in Fig. 80.3(a), and the two normalized waveguide modes are shown in Fig. 80.3(b).

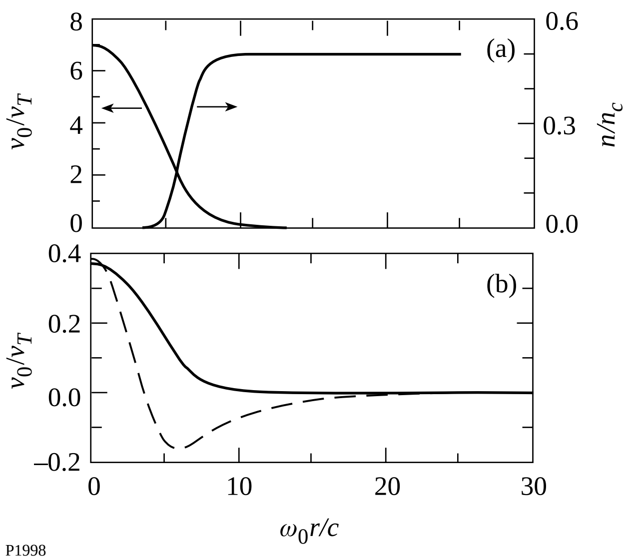

Figure 80.3
(a) Self-consistent equilibrium field and density profiles for a filament with background plasma density $n_0/n_c = 0.5$ and central intensity $v_0/v_T = 7$; (b) the two normalized bound eigenmodes for this filament.

The temporal growth rates and real frequencies for perturbations having the form of the fundamental eigenmode are shown in Figs. 80.4(a) and 80.4(b), plotted against the normalized axial wave number κ. The group velocity of the perturbation normalized to the sound speed can be obtained from the slope of the real frequency curve in Fig. 80.4(b) and, as expected, is near the speed of light: $v_g/c_s \cong 900$ (recall $c/c_s = 1000$ in this example). Thus, a perturbation will propagate along the filament at nearly the speed of light as it grows, leading to a spatial growth rate that can be estimated by dividing the temporal growth rates in Fig. 80.3(a) by $v_g/c_s \cong 900$. This spatial growth rate is quite small, of order $10^{-4}\,\omega_0/c$. For a typical laser-fusion experiment wavelength of 0.351 μm, for example, a small perturbation to a filament could propagate for several thousand microns before becoming large enough to disrupt the filament. Laser-produced plasmas of interest are generally much smaller than this, so that small filaments (radius < one wavelength) are effectively stable to perturbations of this form.

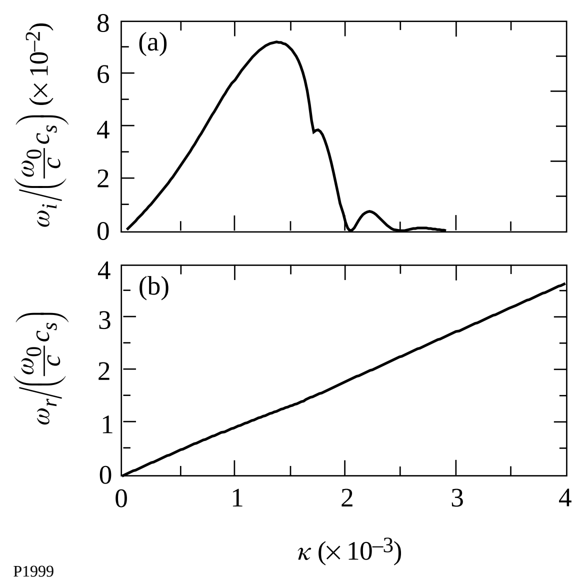

Figure 80.4
Growth rates (a) and real frequencies (b) for perturbations in the form of the fundamental eigenmode (solid line) in Fig. 80.3(b).

The situation is more interesting for filaments large enough that two or more waveguide modes will propagate. Figures 80.5(a) and 80.5(b) show the temporal growth rate and real frequency for the perturbation corresponding to the second waveguide mode for the same filament parameters as in Fig. 80.4. Note that the growth rate is now considerably larger, but more significant is the fact that the axial wave number of the perturbation (given by the difference in the two waveguide-mode wave numbers) is much larger than in the single-mode case. This makes the group velocity [Fig. 80.5(c)] at which the perturbation propagates much smaller, and the resulting spatial growth rate much larger. This effect is due to the fact that having two different dispersion relations for the interacting modes allows larger values of Δk for a given $\Delta\omega$. More importantly, however, the fact that the group velocity in Fig. 80.5(c) passes through zero suggests the possibility of an absolute instability, which grows without propagation. If we define $\kappa_{\max}$ to be the value of κ for which the temporal growth rate in Fig. 80.5(a) is a maximum, and $\Omega_{\max}$, $\Omega'_{\max}$, $\Omega''_{\max}$ to be the corresponding frequency and its first and second derivatives with respect to κ, the condition for absolute instability is[12]

$$\mathrm{Im}\left(\Omega_{\max}\right) > \frac{1}{2}\left(\Omega'_{\max}\right)^2 \mathrm{Im}\left(\frac{1}{\Omega''_{\max}}\right).$$

Evaluation of these quantities shows that this condition is well satisfied (the left side in this example is 0.164, and the right is 0.047), so that the instability is indeed absolute. This means

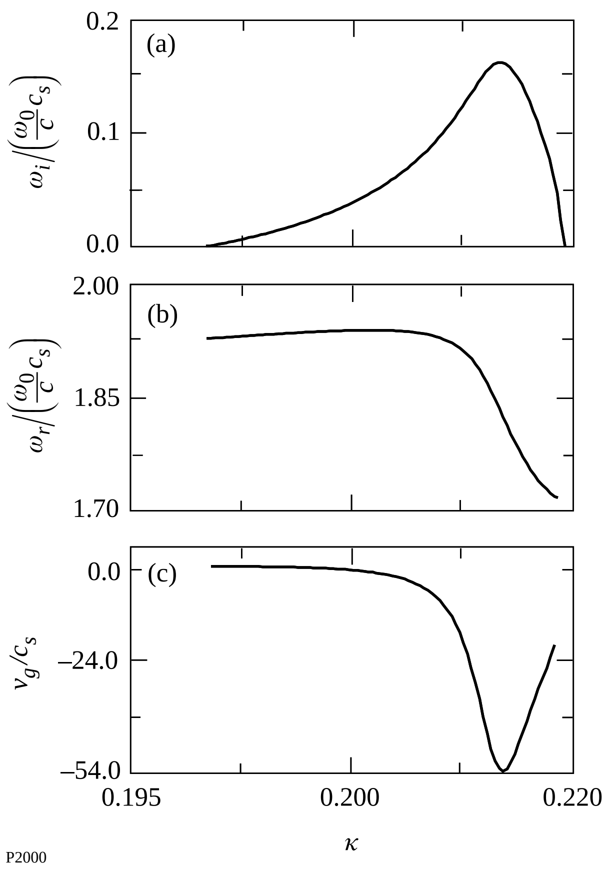

Figure 80.5
Growth rates (a), real frequencies (b), and group velocities (c) for perturbations in the form of the second eigenmode (dashed line) in Fig. 80.3(b).

that the perturbation will remain in place as it grows, rather than propagating along the filament. Unless saturated by some nonlinear mechanism, such an instability would be expected to quickly disrupt the filament.

When the filament is large enough that many modes will propagate, one approaches a "classical" regime where the propagating light may be treated by the paraxial approximation or ray tracing. From the above analysis it is expected that such filaments would be unstable, which seems to be the case in simulations.[7,8]

The above stability analysis has been concerned with a sausage-type perturbation, i.e., one with no azimuthal variation in the cylindrical coordinates centered on the equilibrium filament. "Kink-type" modes, with nonvanishing azimuthal wave numbers, could be treated using a straightforward extension of the above analysis. Such modes would, of course, require a filament large enough to carry these higher-order modes, so small single-mode filaments would be unaffected. Larger filaments could be unstable to both kink and sausage perturbations; which one dominates in practice is a subject for further research. Another topic requiring further study is the effect of plasma inhomogeneity, though by analogy with other wave–plasma interactions, inhomogeneity might be expected to reduce instability growth rates.

In conclusion, the first analysis of filament stability using a realistic self-consistent filament equilibrium and a wave-equation treatment of light propagation has been carried out using a semi-analytic approach. It is found that small filaments that carry light in only one waveguide mode have only a weak convective instability and, in most cases of interest in laser–plasma interactions, may be regarded as essentially stable. Filaments large enough to carry two or more waveguide modes are unstable to sausage-type perturbations, which can be absolutely unstable and may lead in typical cases to distortion or breakup of the filament within a few tens of microns.

ACKNOWLEDGMENT

This work was supported by the U.S. Department of Energy Office of Inertial Confinement Fusion under Cooperative Agreement No. DE-FC03-92SF19460, the University of Rochester, and the New York State Energy Research and Development Authority. The support of DOE does not constitute an endorsement by DOE of the views expressed in this article.

REFERENCES

1. P. Kaw, G. Schmidt, and T. Wilcox, Phys. Fluids **16**, 1522 (1973).
2. D. E. Hinkel *et al.*, Phys. Plasmas **5**, 1887 (1998).

3. D. E. Hinkel, E. A. Williams, and C. H. Still, Phys. Rev. Lett. **77**, 1298 (1996).

4. T. Afshar-rad *et al.*, Phys. Fluids B **4**, 1301 (1992).

5. R. W. Short, W. Seka, and R. Bahr, Phys. Fluids **30**, 3245 (1987).

6. R. W. Short and A. Simon, Phys. Plasmas **5**, 4134 (1998).

7. A. J. Schmitt and B. B. Afeyan, Phys. Plasmas **5**, 503 (1998).

8. F. Vidal and T. W. Johnston, Phys. Rev. Lett. **77**, 1282 (1996).

9. E. Valeo, Phys. Fluids **17**, 1391 (1974).

10. E. J. Valeo and K. G. Estabrook, Phys. Rev. Lett. **34**, 1008 (1975).

11. W. L. Kruer, *The Physics of Laser–Plasma Interactions*, Frontiers in Physics, Vol. 73, edited by D. Pines (Addison-Wesley, Redwood City, CA, 1988).

12. L. S. Hall and W. Heckrotte, Phys. Rev. **166**, 120 (1968).